A 3D gravity data interpretation of the Matagami mining camp, Abitibi Subprovince, Superior Province, Québec, Canada. Application to VMS deposit exploration

Pierre Boszczuk, Li Zhen Cheng, Hanafi Hammouche, Patrice Roy, Sylvain Lacroix, Alain Cheilletz

▶ **To cite this version:**

Pierre Boszczuk, Li Zhen Cheng, Hanafi Hammouche, Patrice Roy, Sylvain Lacroix, et al.. A 3D gravity data interpretation of the Matagami mining camp, Abitibi Subprovince, Superior Province, Québec, Canada. Application to VMS deposit exploration. Journal of Applied Geophysics, 2011, 75, pp.77-86. 10.1016/j.jappgeo.2011.06.031 . insu-03619290

HAL Id: insu-03619290

https://insu.hal.science/insu-03619290v1

Submitted on 10 May 2023

HAL is a multi-disciplinary open access archive for the deposit and dissemination of scientific research documents, whether they are published or not. The documents may come from teaching and research institutions in France or abroad, or from public or private research centers.

L'archive ouverte pluridisciplinaire **HAL**, est destinée au dépôt et à la diffusion de documents scientifiques de niveau recherche, publiés ou non, émanant des établissements d'enseignement et de recherche français ou étrangers, des laboratoires publics ou privés.

A 3D gravity data interpretation of the Matagami mining camp, Abitibi Subprovince, Superior Province, Québec, Canada
Application to VMS deposit exploration

Pierre Boszczuk [a,*], Li Zhen Cheng [b,1], Hanafi Hammouche [c,2], Patrice Roy [d,2], Sylvain Lacroix [e,2], Alain Cheilletz [f,3]

a Ecole Nationale Supérieure de Géologie ENSG-INPL Nancy Université and Centre de Recherches Pétrographiques et Géochimiques, 15 rue Notre Dame des Pauvres, 54501, Vandoeuvre-lès-Nancy, France
b Université du Québec en Abitibi-Témiscamingue, 445 boulevard de l'Université, Rouyn-Noranda, Québec, Canada J9X 5E4
c Bureau de l'Exploration Géologique du Québec, Ministère des Ressources naturelles et de la Faune, 400 boulevard Lamaque, Val-d'Or, Québec, Canada J9P 3L4
d Direction générale de Géologie Québec, Ministère des Ressources naturelles et de la Faune, 400 boulevard Lamaque, Val-d'Or, Québec, Canada J9P 3L4
e Bureau de l'Exploration Géologique du Québec, Ministère des Ressources naturelles et de la Faune, 400 boulevard Lamaque, Val-d'Or, Québec, Canada J9P 3L4
f Ecole Nationale Supérieure de Géologie ENSG-INPL Nancy Université and Centre de Recherches Pétrographiques et Géochimiques, 15 rue Notre Dame des Pauvres, 54501, Vandoeuvre-lès-Nancy, France

Two inversions, unconstrained and constrained, of a gravity survey of the Matagami mining camp (Abitibi Archaean Subprovince, Canada) have been performed in order to identify the downward extension of a rhyolitic horizon hosting VMS-type base metals deposit and the morphologies of the major felsic plutons. A comparative study exhibits the similarities between measured and calculated densities from chemical compositions of the Matagami lithologies. This allows building an initial 3D geodensity model which integrates densities and available structural and geological surface mapping data. This model is integrated during the iteration process of the constrained inversion in the objective function. The resulting true density model and two derived cross-sections upgrade the 3D imaging of this area. Also, the model gives new insight for regional geological interpretation exposing possible shapes of the main geological units at depth and suggests the potential existence of deep fertile geological bodies.

1. Introduction

Searching for deep exploration targets is one of the main issues in mining industry today, as easily detectable ore bodies become rarer. In order to constrain the shape of geological bodies at depth, gathering maximum information from geophysical data interpretations (for example gravity or magnetism) is becoming more and more important. This goal is also supported by the strong development of software and platforms that are able to integrate a large set of geoscientific and technical data.

The Matagami mining camp is located in the North of the Abitibi Archean greenstone belt (Goutier and Melançon, 2007) in the Superior Province, which is the largest Archean craton in the world. The mined VMS-type Zn–Cu–Ag–Au deposits are hosted at the top of the rhyolitic horizon of the Watson Lake Group (WLG), which constitutes the base of the volcanic stratigraphic sequence (Piché et al., 1993), in the direct neighborhood of the Key Tuffite exhalite, a cherty sulfidic marker horizon. The upper volcanic horizons of the Wabassee Group are essentially composed of basalts and andesites. In this area, exploration of VMS-type deposits yields to the opening of 11 mines, for example the largest Mattagami Lake Mine (total production 25.64 Mt ore at 8.2% Zn, 0.56% Cu, 20.91 ppm Ag and 0.41 ppm Au). The Perseverance Mine started its production in 2008 and is today the only active site. Considering its significance as a lithological marker for VMS discoveries, this paper aims to delineate the extension at depth of the WLG rhyolitic horizon using gravity inversions constrained by new density data from recent geological fieldwork.

Magnetic and gravity surveys within the Matagami mining camp were performed in 2007 by the Geological Survey of Canada (GSC), the Bureau de l'Exploration Géologique du Québec (BEGQ) and several active mining companies (Xstrata, SOQUEM). Public regional geophysical data considered in this study are: (1) the aeromagnetic survey DP-2006-07 (Ministère des Ressources Naturelles et de la Faune, MRNF, 2006) and (2) the ground gravity survey DP-2007-01 (MRNF, 2007). Previously,

* Corresponding author. Tel.: +33 6 76 44 47 55.
E-mail addresses: pierre.boszczuk@hotmail.com (P. Boszczuk), li_zhen.cheng@uqat.ca (L.Z. Cheng), hanafi.hammouche@mrnf.gouv.qc.ca (H. Hammouche), patrice.roy@mrnf.gouv.qc.ca (P. Roy), sylvain.lacroix@mrnf.gouv.qc.ca (S. Lacroix), cheille@crpg.cnrs-nancy.fr (A. Cheilletz).
[1] Tel.: +1 819 762 0971x2351.
[2] Tel.: +1 819 354 4514.
[3] Tel.: +33 3 83 59 42 33.

some acquisition of regional geological infrastructures (Hammouche et al., 2008, 2010; and Rhéaume, 2009, 2010) and geophysical interpretation (Adam et al., 1998; and Calvert and Li, 1999) aimed to rebuild the deep structure in the Matagami area, and to elaborate a relative chronology between different geological units according to their occurrence at depth (Lacroix et al., 1990). However the deep extension of the WLG rhyolitic horizon is still unclear.

The inversion method of potential-field data has been widely applied in mining exploration and in solving environmental problems. A number of methods and optimization algorithms have been used for gravity data inversion such as Gauss–Newton methods (Barbosa and Silva, 1994), finite-difference solution of Poisson's equation (Farguharson and Mosher, 2009) or Monte Carlo methods (Bosch et al., 2006).

However the inversion problem remains underdetermined and numerous possible density distribution models appear satisfying the observations. In order to reduce the nonuniqueness of the solution some authors added constraints to the inversion algorithm. Boulanger and Chouteau (2001) focused on the minimum curvature, flatness, compactness (also developed by Last and Kubik, 1983) and smoothness properties of the generated bodies. Guillen and Menichetti (1984) minimized the moment of inertia of the anomalous sources considering the centers of gravity or given dips; Barbosa and Silva (1994) incorporated a priori information about the maximum compactness of the sources; Silva and Barbosa (2006) and later Silva Dias et al. (2009) defined the assumed outline of the gravity sources and refined them through the inversion process. More recently, a cokriging stochastic approach was proposed by Chasseriau and Chouteau (2003) and Shamsipour et al. (2010). For a review of the stabilizing constraints used in inversion methods, see Silva et al. (2001).

In our study, we chose the constrained inversion method of Li and Oldenburg (1998) that minimizes a function composed by (1) the data-misfit function defined in the data space as the L2 norm of the difference between the observed and predicted data, and (2) the stabilizing function defined in the parameter model space as the L2 norm of the first-order derivative of the weighted density distribution in both vertical and horizontal directions. Our work also involves direct density determinations and structural geology measurements in the field. This information is integrated into an initial 3D density model which reflects the geological reality of the Matagami mining camp. This preliminary model was then incorporated in the inversion procedure. A meaningful geologic model from this constrained inversion is finally presented.

2. Geological context

The Matagami mining camp is bounded at its NW corner by the Matagami shear zone and at the SW corner by the Taïbi-Nord and Casa-Berardi shear zones (Daigneault, 1996). These tectonic lineaments were plotted using ground field data and interpretations of the geophysical surveys. In the Matagami mining camp, the volcanic sequences are constituted by the felsic rocks of the Watson Lake Group (WLG) which host the VMS-type deposits and the intermediate to mafic volcanic rocks of the Wabassee Group (Fig. 1). The Key Tuffite, a 0.6 m to 6 m cherty sulfidic horizon, usually marks the contact between the WLG and the upper Wabassee Group. This thin horizon constitutes a historic exploration target because most of the deposits discovered in the area are located in its neighborhood (Calvert and Li, 1999). The base of the WLG is intersected by the mafic Bell River intrusive Complex (2 725 ± 3 Ma, Mortensen, 1993) which consists of 80% gabbro. There is a great heterogeneity in composition within the Bell River Complex as revealed by the magnetic anomaly images (Fig. 2). The other major intrusive rocks in the study area are: (1) the McIvor Pluton (2 724 ± 7 Ma) interpreted as synvolcanic by Rhéaume (2010) that varies in composition from tonalitic to dioritic, and (2) the felsic Cavelier Pluton located in the south. A high-magnetic ring indicates a metamorphic halo around the Cavelier Pluton (Fig. 2). It is probably related to the postvolcanic character of the pluton (Lacroix et al., 1990). Several intermediate to ultramafic Archean intrusions and Proterozoic subvertical diabase dykes, with a N065 mean orientation, crosscut the volcanic sequences. These are characterized by high-magnetic anomalies.

The Galinée Anticline is a major regional structural feature (Figs. 1 and 3; Beaudry and Gaucher, 1986; Hammouche et al., 2010; Rhéaume,

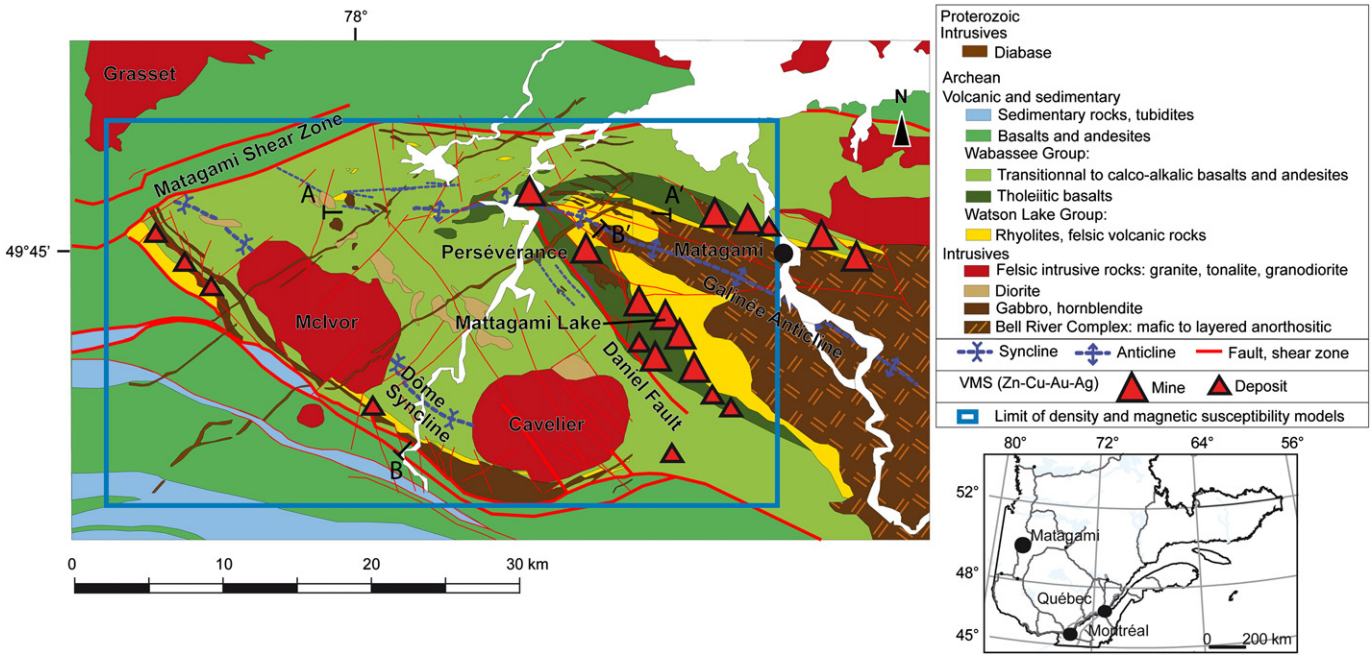

Fig. 1. Geological map of the Matagami mining camp showing main lithological units, location of the study area for gravity and magnetism inversions and location of the sections of Fig. 3 (A–A′) and (B–B′). The modeled area is indicated by the blue line on the geological map.
Central area mapping modified from Hammouche et al. (2010) and Rhéaume (2010); eastern area mapping modified from Piché et al. (1993). Regional sheared structures modified from Goutier and Melançon (2007).

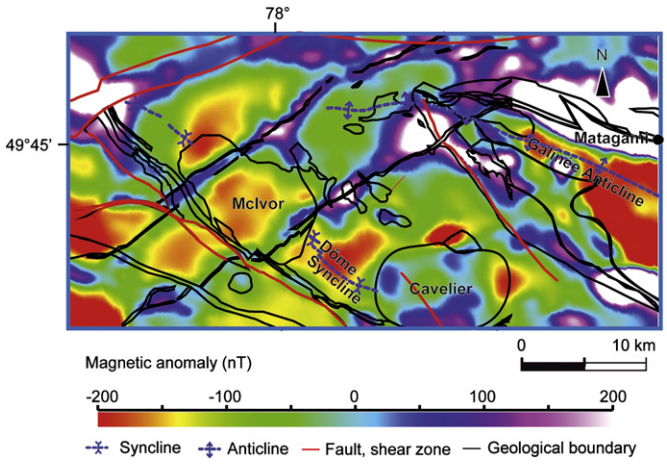

Fig. 2. Map of the residual magnetic anomaly obtained after removal of a second order polynomial trend from the MRNF DP-2006-07 aeromagnetic survey. The Proterozoic magnetite rich diabase dykes, appear at the regional scale. The limits of major lithologies and structures extracted from the geological map of Fig. 1 are also represented.

2010). From East to West its axis shows a SE–NW orientation turning to East–West in the center of the area. Volcanic sequences dipping 80° to the North on the northern flank of the anticline and 45° to the South on the southern flank (Fig. 3; Piché et al., 1993). It is generally admitted that the axis of the Galinée Anticline has a general plunge to the NW at its

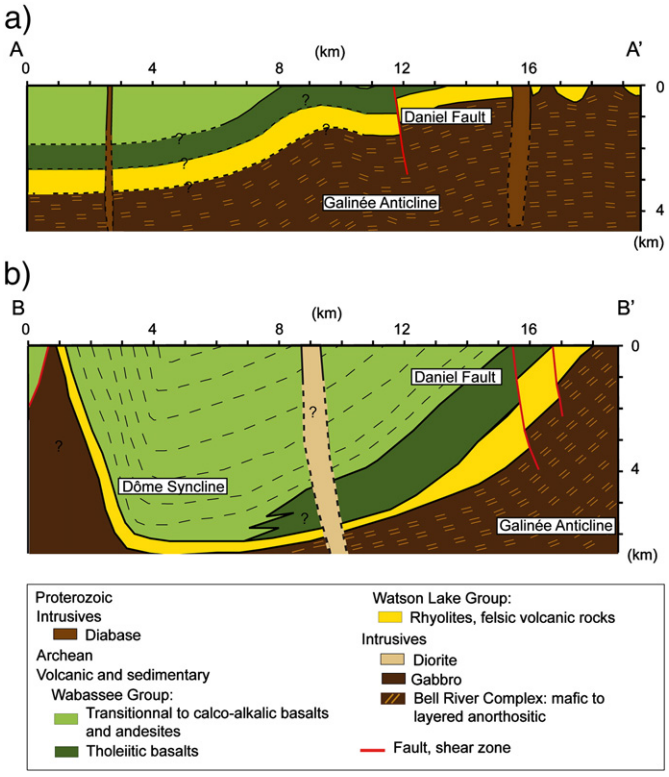

Fig. 3. Cross sections of the Matagami mining camp (see Fig. 1 for localizations). The 45° dip of the Watson Lake Group rhyolitic horizon on the Southern flank of the Galinée Anticline is established by Piché (1991) and geological cross sections of historical mines. The dip of the Daniel Fault and its 500 m vertical throw are calculated from seismic reflection interpretation (Adam et al., 1998) a) E–W section parallel to the Galinée Anticline plunging axis. The presence in the middle of the section of tholeiitic basalts, characterizing the base of the Wabassee Group sequence, would imply a local bend of the anticline axis. b) SW–NE section perpendicular to the southern flank of the Galinée Anticline exemplifying the postulated Dôme Syncline.
The geological horizons and structure locations are obtained from the Hammouche et al. (2010) and Rhéaume (2010) geological maps.

NW extremity. Nevertheless, local waving of the anticline axis could provoke the outcropping of the underlying tholeiitic basalts of the Wabassee Group, usually located directly on the top of the WLG rhyolitic horizon (Hammouche et al., 2010). A second postulated major structural feature is the Dôme Syncline (Fig. 1; Rhéaume, 2010). The formation of this syncline could cause the exposure of the WLG rhyolitic horizon at the southern edge of the McIvor Pluton. Since this rhyolitic horizon is also enriched in VMS-type mineralization, it opens regional exploration towards the southern part of the Matagami camp. An important structural element is represented by the NW Daniel Fault (Fig. 1), which intersects the WLG on the southern flank of the Galinée Anticline. It is mainly characterized by a reverse fault, highly dipping to the NE, with at least a 500 m vertical offset, calculated from seismic reflection interpretation (Adam et al., 1998).

3. Real density values

3.1. Real density measurement

The intrinsic link between geological and geophysical data is the physical properties of the rocks. As in many other geophysical methods, the inverse problem of estimating a discrete density distribution from the gravity anomaly is an ill-posed problem. In other words, more than one density distribution can give a similar geophysical response. To reduce this ambiguity, prior information about physical properties and geology must be used. Thus we decided to perform density measurements on 373 samples collected in the Matagami area (Table 1 and Fig. 4) representing 226 outcrop samples collected during the BEGQ Matagami geological mapping campaign in 2008. Additionally, 147 core samples were provided by Xstrata Zinc.

The analytical procedure for density measurement consists of a standard wet and dry weighting of hand-sized samples. Samples were prepared by removing altered surfaces, cleaning and drying. The electronic balance used for density measurements has a precision p_D of 0.1 g for dry condition and p_W of 0.3 g for underwater measurements. The balance is calibrated every hundred measurements. At every 30 measures, a density measurement on a 5 000 g standard with a density of 7.85 g/cm^3 allows the definition of a correction factor f_c, which limits the impact of the main environmental error sources. Between two standard density measurements, this correction factor is considered to evolve linearly. An electronic thermometer is used to measure underwater temperature in order to calculate the density correction factor f_T (Lide, 2010).

The general density ρ calculation equation is:

$$\rho = \frac{M_D}{M_D - M_W} * f_c * f_T \tag{1}$$

where M_D is the dry mass of the sample and M_W the equivalent immerged mass. Relative error e on the density measurement can be calculated as:

$$e = \frac{\left| \frac{M_D + p_D}{(M_D + p_D) - (M_w + p_W)} * f_c * f_T - \rho \right|}{\rho}. \tag{2}$$

The results of density measurement are presented in Fig. 4. In the Matagami mining camp area the mean values of measured densities of basalts and andesites are very close, i.e. 2.87 g/cm^3 and 2.88 g/cm^3, respectively. Table 1 shows the statistical analysis of the measured densities from the Matagami mining camp. Although most of the different lithologies are overlapping between the maximum and minimum values, the 1st and 3rd quartile range allows discrimination between felsic and intermediate to mafic rocks (Fig. 4). In fact, the density similarity between basalts and andesites can be explained by the presence of numerous quartz–epidote amygdules (up to 20%) due

Table 1
Statistics for the measured densities of 373 samples collected in the Matagami mining camp (226 outcrop samples and 147 core samples).

	Mean density (g/cm^3)	Median density (g/cm^3)	1st quartile (g/cm^3)	3rd quartile (g/cm^3)	Minimum density (g/cm^3)	Maximum density (g/cm^3)	Standard deviation on density (g/cm^3)	Mean density measurement relative error	Maximum density measurement relative error	Number of samples
Basalt	2.87	2.85	2.80	2.92	2.70	3.13	0.09	0.25%	1.02%	61
Andesite	2.88	2.87	2.82	2.92	2.69	3.13	0.09	0.38%	1.36%	173
Felsic volcanic rocks	2.75	2.74	2.72	2.77	2.66	2.92	0.05	0.23%	0.91%	57
Mafic intrusive rocks	2.92	2.90	2.85	3.00	2.71	3.09	0.09	0.29%	0.84%	48
Intermediate intrusive rocks	2.80	2.77	2.74	2.83	2.68	3.01	0.08	0.26%	0.83%	25
Felsic intrusive rocks	2.75	2.75	2.72	2.78	2.51	3.02	0.13	0.26%	0.61%	9
Total	2.86	2.85	2.78	2.92	2.51	3.13	0.10	0.32%	1.36%	373

to the filling of primary vesicles during the penetrative hydrothermal alteration episode. This alteration widely affects both basaltic and andesitic lithologies and induces a density homogenization effect. This makes it impossible to distinguish between them using gravity data only. However, considering the interquartile range (Table 1), the felsic lithologies, such as the WLG rhyolites, show lower densities (2.75 ± 0.036 g/cm^3) compared to other volcanic lithologies such as basalts and andesites (2.87 ± 0.066 g/cm^3 and 2.88 ± 0.060 g/cm^3). Therefore, due to a sufficient density contrasts between felsic and mafic lithologies, we are able to use a gravity inversion method for the 3D geological interpretation of the Matagami mining camp.

3.2. Chemical composition of rocks and density calculation

The density measurements on 72 outcrop samples are then compared to calculated densities using the normative calculation program NORMAT® (Piché and Jebrak, 2004) based on the chemical composition of the rocks (Table 2.). The comparison between calculated and measured densities (Fig. 5) displays a linear relationship, with a strong correlation coefficient of 0.974. The slope of the regression line is of 0.993 due to a very good consistency between density measurements and normative calculations. Therefore, the densities estimated from the chemical compositions of rocks are fairly precise and can be used for various applications, including gravity modeling. This results as the generation of a density database from 24607 regional available chemical analyses, namely 371 outcrop samples and 24236 core samples (see location in Fig. 6). The compilation of measured and calculated density is used for the constrained gravity data inversion of the present study. As a consequence of the existence of this large density database, we were able to calculate the mean density value for the Matagami mining camp by weighting the relative proportion of the samples in each lithology. The resulting value is 2.88 g/cm^3.

4. Three dimensional gravity data interpretation

4.1. The Bouguer and residual anomalies

The ground gravity survey extended over 575 km^2 of land, and 402 measurements were collected at the resolution of 500 m (DP-2007-01), from October 2006 to March 2007, using three Lacoste and Romberg gravimeters. The precision of the measurement locations is estimated at ± 1 m in the horizontal plane and at ± 0.5 m along the vertical axis.

The Bouguer anomaly (Fig. 7a) was obtained after: (1) subtraction of the theoretical value of gravity from the observed data, based on the 1980 Geodetic Reference System (the effect of latitude is removed); (2) using a vertical gradient of 0.3086 mGal/m to correct for the effect of elevation on gravity at the station; and (3) considering an average crustal density of 2.67 g/cm^3 to remove the attraction of materials between the observation point and the mean sea level. The Bouguer anomaly precision is estimated at ± 0.17 mGal. No terrain correction was applied as the study area consists mostly in a flat surface.

The Bouguer anomaly grid is reduced to a spacing of 100 m using a minimum curvature gridding algorithm. The residual Bouguer anomaly which outlines the surface geology features is obtained after removing a second order polynomial trend to the Bouguer anomaly (Fig. 7b). Both Cavelier and McIvor felsic plutons are characterized by low gravity areas. The elongated shape of the geological contact between the WLG rhyolites and the Wabassee Group (andesites and basalts) is well marked along the Galinée Anticline.

4.2. The gravity inversion method

Inversions of the gravity field in the Matagami mining camp are processed by UBC-GIF GRAV3D® program following the method described below (Li and Oldenburg, 1998). In a Cartesian coordinate system having its origin on the earth's surface and the z-axis pointing vertically downward, the study area is discretized by a 3D mesh model with M prismatic cells. The gravity data d_i at the ith location of N points of gravity observation can be written as:

$$d_i = \sum_{j=1}^{M} \rho_j \left(\gamma \int_{\Delta V_j} \frac{z - z_0}{\left| \vec{r} - \vec{r}_{0i} \right|^3} dv \right) = \sum_{j=1}^{M} \rho_j G_{ij} \qquad (3)$$

where ρ_j and ΔV_j are the density and volume of the jth cell, $\left| \vec{r} - \vec{r}_{0i} \right|$ is the distance between the center of the ith cell and the observation location and γ is the gravitational constant.

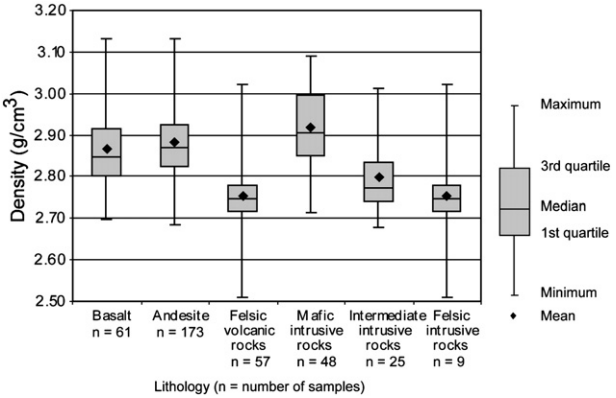

Fig. 4. Box and whisker plots calculated on the measured densities for 373 samples collected on the Matagami mining camp (226 outcrop samples and 147 core samples).

Table 2
Statistics for the calculated densities from chemical analysis of 72 ground samples collected in the Matagami mining camp.

	Mean density (g/cm^3)	Median density (g/cm^3)	1st quartile (g/cm^3)	3rd quartile (g/cm^3)	Minimum density (g/cm^3)	Maximum density (g/cm^3)	Standard deviation on density (g/cm^3)	Mean relative error between measured and calculated density	Maximum relative error between measured and calculated density	Number of samples
Basalt	2.91	2.85	2.84	2.96	2.80	3.13	0.13	1.14%	2.10%	6
Andesite	2.87	2.87	2.82	2.92	2.70	3.10	0.08	0.63%	2.26%	44
Felsic volcanic rocks	2.80	2.81	2.76	2.85	2.71	2.87	0.07	0.55%	1.26%	4
Mafic intrusive rocks	2.91	2.88	2.85	2.99	2.84	3.01	0.07	1.21%	2.24%	13
Intermediate intrusive rocks	2.89	2.90	2.80	2.99	2.70	3.01	0.13	1.03%	3.23%	4
Felsic intrusive rocks	2.75	2.75	2.75	2.75	2.75	2.75		0.02%	0.02%	1
Total	2.88	2.86	2.82	2.93	2.70	3.13	0.09	0.79%	3.23%	72

Mathematically, following Li and Oldenburg's method (1998), the inverse problem consists in minimizing the model and data misfits together. The model-misfit function ϕ_m defined as the difference between the density model obtained at an inversion step and an initial reference model can be expressed as the following:

$$\phi_m(\rho) = \alpha_s \int_V w_s w^2(z)(\rho-\rho_0)^2 dv + \alpha_x \int_V w_x \left(\frac{\partial w(z)(\rho-\rho_0)}{\partial x}\right)^2 dv + \alpha_y \int_V w_y \left(\frac{\partial w(z)(\rho-\rho_0)}{\partial y}\right)^2 dv + \alpha_z \int_V w_z \left(\frac{\partial w(z)(\rho-\rho_0)}{\partial z}\right)^2 dv \quad (4)$$

where ρ_0 is a vector characterizing the density of the reference model; w_s, w_x, w_y, and w_z are weighting functions and $w(z)$ is the depth-weighting function. $\alpha_s, \alpha_x, \alpha_y$, and α_z are coefficients which affect the relative importance of the different components. The data-misfit functionφ_d is the L2-norm of the weighted difference between the gravity observation d_{obs} and the predicted gravity response d_{mod}:

$$\phi_d = ||W_d(d_{\mathrm{mod}} - d_{obs})||^2 \quad (5)$$

where W_d is a diagonal matrix of which the ith element is the standard deviation of the ith datum. The inversion process aims to minimize the function ϕcomposed of both model and data misfit functions until a threshold is reached:

$$\phi = \phi_d + \mu\phi_m \quad (6)$$

where μ is a regularization parameter. The minimization of the objective function ϕ is subject to $\rho_{\min} \le \rho \le \rho_{\max}$ where $\rho_{\min}$ and $\rho_{\max}$ are the lower and upper bounds on the density contrast.

We divided our study area into 4825212 cubic cells with a cell size of 100 m. The density model is 43 km long from the East to the West, 21.6 km from the North to the South and 5 km from the top to the bottom. In general, three key factors should be considered in an inversion: (1) defining the upper and lower bounds on the density contrast which allows inversion to quickly converges; (2) defining weighting function to emphasize the variation of physical property on a specific direction; and (3) defining length scales for the smoothness of the model $L_x = \sqrt{\alpha_x / \alpha_s}$, $L_y = \sqrt{\alpha_z / \alpha_s}$ and $L_z = \sqrt{\alpha_z / \alpha_s}$. The UBC research group defined default values based on numerous tests and they are convenient in the most cases. We used $\rho_{\min} = -2.00$ g/cm^3 and $\rho_{\max} = 2.00$ g/cm^3 as lower and upper bounds of the density contrast since the residual Bouguer anomalies are mixed negative and positive. We need to adjust weighting functions w_s, w_x, w_y, and w_z only if we know the true geological structure and we would like to emphasize its importance. We do not have such accurate information at depth in the studied region therefore we used the default values. We used the default value for the three length scales which are two times the maximum cell width.

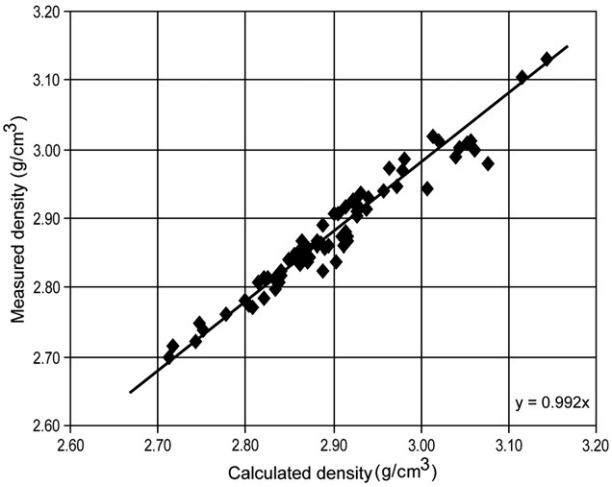

Fig. 5. Cross plot of measured densities and calculated densities from chemical analysis on 72 samples collected during the 2008 BEGQ Matagami mapping field campaign. The correlation coefficient is 0.974. The slope of the line obtained by linear regression is 0.993. Mean absolute error between calculated and measured densities (error type) is 0.020.

A null density is applied to the cells whose centers are located above the topographic surface obtained from Geological Survey of United States (USGS) database. Those data were collected through the

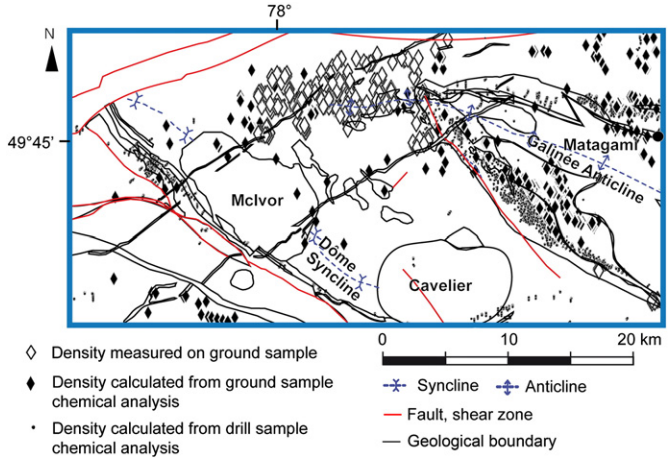

Fig. 6. Location of ground and core samples used for density measurement and normative density calculations. The limits of major lithologies and structures extracted from the geological map of Fig. 1 are also represented.

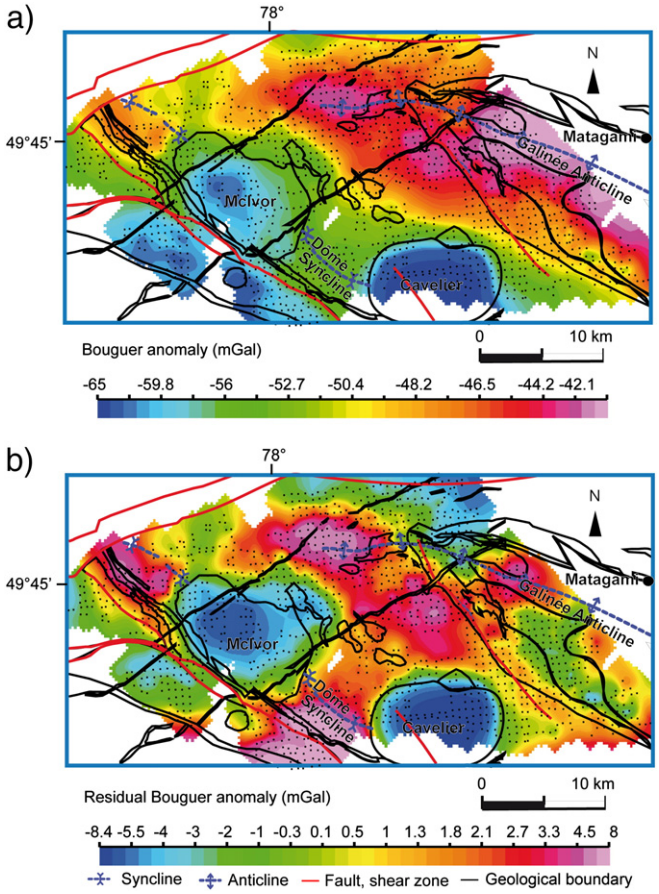

Fig. 7. a) Map of the Bouguer anomaly from the MRNF DP-2007-01 gravity survey. b) Map of the residual Bouguer anomaly obtained after removal of a second order polynomial trend. The main low density geological bodies, like the McIvor and Cavelier plutons appear. The limits of major lithologies and structures extracted from the geological map of Fig. 1 are also represented.

Shuttle Radar Topography Mission (SRTM) and were processed by NASA and NIMA at 3 arc-seconds. The resolution is about 90 m.

In the Matagami mining camp, the overburden is principally composed of deep water sediments, clay, silt, sand and organic deposits (Veillette and Pomares, 2003). The thickness of the overburden is estimated by 5376 drillholes from the Système d'Information GÉOMinière (SIGEOM)-MRNF database (Fig. 8). Following the literature (Telford et al., 1990), the density of those sediments varies from 2.30 g/cm^3 to 2.60 g/cm^3. Taking into account the presence of basic lithologies in numerous pebbles of the Quaternary detrital sediments, we considered a mean density of 2.50 g/cm^3 for the forward modeling. The impact to the gravity field from the overburden is 0.24 mGal on average with a 1.19 mGal maximum. For 90% of the study area this impact is less than 0.51 mGal. Therefore, the effect of the overburden on gravity modeling is minor.

4.3. Results from an unconstrained inversion

The model obtained from the unconstrained inversion, which consists in minimizing the data-misfit function (Eq. 5) setting W_d equal to the identity matrix, is shown on the Fig. 9. A good agreement results when comparing the density sub-surface distribution with the geological limits of the Cavelier and McIvor plutons at the southern and western margins. The isodensity surface presented on Fig. 9a separates the densities higher than 2.87 g/cm^3 (mafic lithologies and andesites), from the lower density zones (felsic lithologies and intermediate intrusives). A horizontal section at the 1 km depth (Fig. 9b) shows the existence of the plutonic bodies at depth. The unconstrained inversion also reveals two low density zones at the northern border (a) and at the eastern boundary (b), which might correspond to the WLG rhyolitic horizon folded by the Galinée Anticline at its western axis prolongation (a) and on its southern flank (b). The rounded low density area in the southeastern corner (c) and the elongated zone (d) are more difficult to interpret without any surface information. This could reflect the presence of sedimentary rocks and turbidites (Fig. 1). A N–S section (profile A–A′, Fig. 9c), allows the distinction of several geological units. From the West to the East, (1) sedimentary and volcanic rocks (SVR) corresponding to a low density area which is in contact with a mafic intrusive body (MIR) characterized by high densities (2.90 g/cm^3 to 2.95 g/cm^3), (2) the complex shape of the McIvor Pluton revealed by low density surfaces (2.73 g/cm^3 to 2.86 g/cm^3) which can be separated at the surface into two individual fingers (MIV and MIE), (3) a high density area corresponding to the Wabassee Group volcanics (WGV), (4) a low density zone (2.84 g/cm^3 to 2.87 g/cm^3) probably representing the Watson Lake Group rhyolites (WLG) and finally, (5) the high density of the Bell River Complex (BRC). On this N–S section, the point (b) indicates that the WLG rhyolitic horizon (low density zone) has a limited extension at depth.

This unconstrained inversion model reveals several important aspects. The low density area that corresponds to the WLG rhyolitic horizon on the southern flank of the Galinée Anticline (at point b) appears to be subvertical. This result is not consistent with field observations as mentioned by Beaudry and Gaucher (1986) and Piché (1991). These authors draw this horizon with a dip of 45° to the SW. A constrained inversion is thus needed to upgrade the 3D model.

Even though the McIvor and Cavelier plutons have a considerable deep extension, their 3D shapes are very distinct. The Cavelier Pluton is likely a vertical cylinder, while the McIvor Pluton's shape is more complex. Was the McIvor Pluton bent with the host rocks by posterior tectonic event? Was it deformed by faults or shear zones? Or does it correspond to the emplacement of two different intrusions? Available hypotheses are that the McIvor Pluton is an early tectonic or synvolcanic intrusion (Lacroix et al., 1990) whereas the Cavelier Pluton is interpreted as a late tectonic intrusion. This could be the reason why the 3D shapes of these two plutons are completely different. Moreover, the Cavalier Pluton is surrounded by a ring of highly magnetic anomalies which could be explained by a contact-metamorphic halo (Fig. 2).

5. The constrained inversion model

5.1. Building the reference model

The usefulness of constraining the inversion is to orient the iterations of the process to a solution in accordance with the

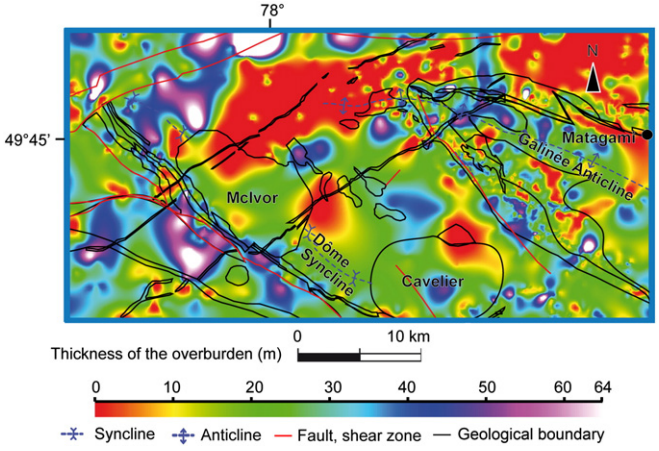

Fig. 8. Map of thickness of the overburden interpolated from 5376 drillholes from the MRNF-SIGEOM database. The limits of major lithologies and structures extracted from the geological map of Fig. 1 are also represented.

geological hypothesis, especially in the case of a horizontal layered structure, where we are not able to separate the gravity signal of one layer from another without prior information.

The constrained inversion procedure starts with a density model integrating the available geological information. We successively consider the regional structural geology features (Daniel Fault, Galinée Anticline and Dôme Syncline), the seismic reflection interpretation along the profile of Fig. 3a (Adam et al., 1998), and the vertical extension of the main geological objects (Proterozoic diabase dykes and Cavelier Pluton) obtained from the preliminary unconstrained inversion of the gravity data (Fig. 9). The 24607 known density points calculated from the chemical compositions of outcrop and drillhole samples are used in two ways: (1) determine the average density for each considered geological body; (2) set the density value to all cells crosscut by drillholes or containing outcrops with measured or calculated density. A Discrete Smooth Interpolation (DSI; Mallet, 1992) is processed to avoid abrupt density contrasts in the reference model (Fig. 10).

Table 3 sums up the geological objects modeled in the reference density model.

5.2. Constrained inversion results

The 3D density-distribution model obtained from constrained inversion is shown in Fig. 11. This model reveals a general geometric distribution of different lithologies in good agreement with the unconstrained inversion results. However, some additional and important information appear (Fig. 11b, c).

The horizontal section (Fig. 11b) delineates a low density rounded anomaly (a) on the southern flank of the Galinée Anticline. This suggests either the break of the WLG rhyolitic horizon in this area or the presence of a felsic intrusion. The low density area (b) at the northern boundary of the WLG opens the discussion about the westward extension of the WLG rhyolitic horizon along the Galinée Anticline axis. The vertical section (Fig. 11c) presents the superposition of the density distribution from constrained inversion and the outline of the reference model (dashed line) used for the constrained inversion. This section presents several improvements compared to the cross-section obtained from the unconstrained inversion (Fig. 9c). From the West to the East: (1) The WLG appears at the western contact of the McIvor Pluton. Its down-dip extension (c) is not yet discernable below the depth of 1 km. (2) The Proterozoic diabase dykes (PDD) are well recovered. (3) By taking into account the shape of the McIvor Pluton from previous studies (Beaudry and Gaucher, 1986; Hammouche et al., 2010), we obtain a local rising at its bottom (d). (4) The WLG on the southern flank of the Galinée Anticline (e) is dipping 45° to the SW, which allows the down-dip extension of this important geological unit to 2 km depth. The offset by the Daniel Fault (DF) is also well apparent.

Additionally, the following elements require a particular concern.

The extension deeper than 2 km of the WLG rhyolitic horizon on the southern flank of the Galinée Anticline is not visible in the density model obtained from constrained inversion, in spite of its integration in the reference model. Even if the WLG rhyolitic horizon exists deeper than 2 km, due to its small volume or to the intrusion of higher density geological bodies, it would be insufficient to produce a detectable anomaly. However, on the southeast part of the southern flank of the Galinée Anticline, the successive constrained inversion iterations yield the visibility of the WLG rhyolitic horizon, but with an overvaluation of the densities of neighboring lithologies.

At the eastern contact of the McIvor Pluton, it is difficult to follow the WLG rhyolitic horizon at depth, for the same reasons as for the southern flank of the Galinée Anticline.

Even if the WLG rhyolitic horizon is extended in the NW of the Galinée Anticline along its plunging axis in the reference model, the constrained inversion generated a low density zone between the top of the referenced rhyolitic horizon and the surface. This may indicate the presence of the WLG rhyolitic horizon at a shallower depth.

6. Discussion

The original inversion gravity method we describe in this work is mainly based on a large density data base acquisition. This is allowed by the strong correlation existing between measured and calculated densities and by the use of the huge available geoscientific information in this area. This allows us to define the real density of the various lithological units represented in the Matagami mining camp and consequently the mean density of the whole area. This careful density

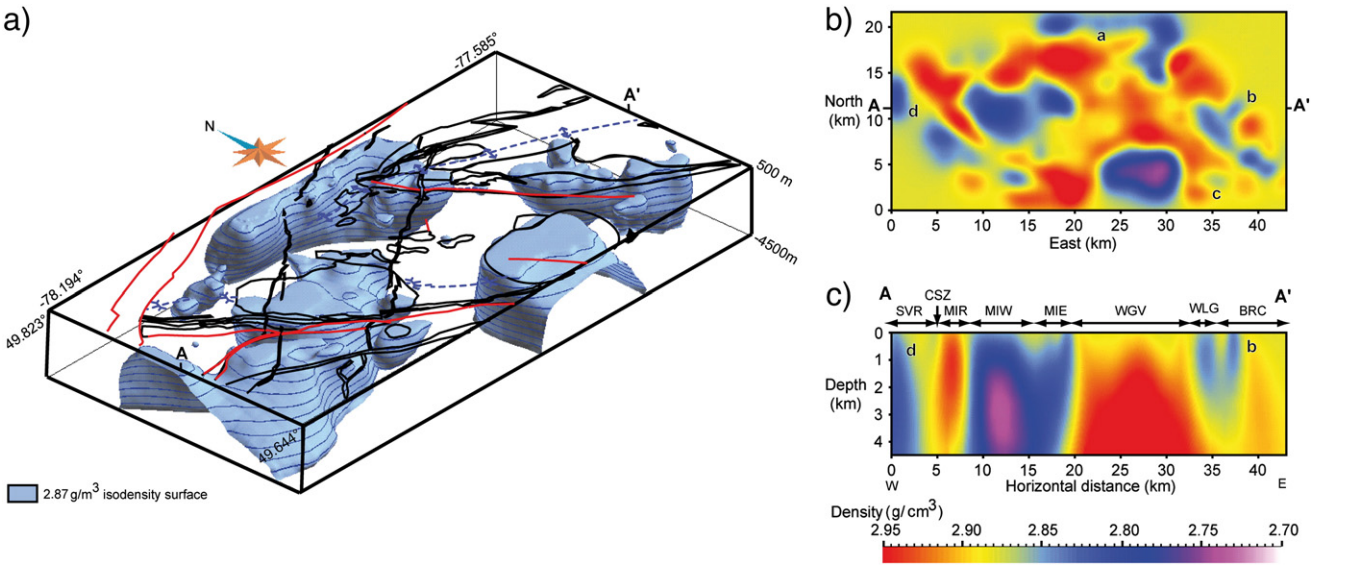

Fig. 9. a) 3D representation of the 2.87 g/cm^3 isodensity surface obtained after unconstrained inversion of the regional gravity anomaly. As the mean density of the studied area is 2.88 g/cm^3, this surface separates the geological objects with a higher density than 2.87 g/cm^3, supposedly mafic lithologies and andesites that provoke positive gravity anomalies, from the objects with a lower density, supposedly felsic lithologies and intermediate intrusives that provoke negative gravity anomalies. The interval between the isobath lines is 500 m. The limits of major lithologies and structures extracted from the geological map of Fig. 1 are also represented. b) Horizontal cross section at the 1 km depth. c) Vertical cross section at 49.741° latitude/78.189° longitude and 49.724° latitude/77.592°longitude. SVR: Sedimentary and Volcanic Rocks. MIR: Mafic Intrusive Rocks. MIW: McIvor Pluton West. MIE: McIvor Pluton East. WGV: Wabassee Group Volcanic rocks. WLG: Watson Lake Group rhyolitic horizon. BRC: Bell River Complex.

analysis makes then possible the discrimination between felsic geological bodies (WLG rhyolitic horizon and felsic plutons) and intermediate to mafic ones (Bell River Complex and Wabassee Group) from a standard gravity survey. Conducted with a multiple disciplinary data set (geology, geochemistry and geophysics), this constitutes the basis of our reference model used for the constrained inversion.

The misfit between observed and predicted gravity anomalies is shown in Fig. 12a for unconstrained inversion and in Fig. 12b for constrained inversion. Obviously both misfits have a normal distribution with the mean value near zero. The standard deviation of the misfit for constrained inversion is 0.10 mGal which is lower than the standard deviation of 0.29 mGal for unconstrained inversion. This demonstrates that the model is improved by the constrained inversion. The density model of the Matagami mining camp obtained by Shamsipour et al. (2010), using stochastic inversion method, is comparable to our model obtained from unconstrained inversion.

Macro- and micro-porosities have not been considered as a parameter able to affect our rock density evaluations. In fact, the comparison between calculated and measured densities (Fig. 5) and the linear relationship (with a regression line slope of 0.993) supports our interpretation of a minor influence of this petrographic feature. Besides, vesicles in rhyolite, andesite and basalt outcrops are commonly observed (Hammouche et al., 2008, 2010; and Rhéaume, 2010) and are typically (up to 20% amygdules) filled with minerals such as quartz or epidote; their contribution was therefore intrinsically taken into consideration through both chemical analysis and density measurements. Due to the lack of information, hypothetic large scale porosity areas (fault zones and alteration areas for instance) are not considered in this study and assumed to be local features which will not modify the density models for our regional geology interpretation.

One major concern of this study was to elucidate the extension at depth of the WLG rhyolitic horizon associated with VMS-type deposits. In the northern part of the study area, both constrained and unconstrained inversions yield density models in which a low density zone exists along the plunging axis of the Galinée Anticline situated immediately at the northern limit of the tholeiitic basalt horizon (Fig. 1). This anomaly is most probably due to the presence of the WLG rhyolitic horizon at depth.

The equivalent source problem in the potential field data interpretation leads to ambiguities. We can see clearly this non-uniqueness of the inversion solutions in the case of the McIvor Pluton: the unconstrained inversion proposes a low density body, which is seemly composed at the surface of two individual fingers (i.e. the NE part and the SW part (Fig. 9)) but when a constrained inversion is processed with a reference model that includes the shape of the pluton drawn by Beaudry and Gaucher (1986) and Hammouche et al. (2010), a local rise of the pluton's base can be observed (Fig. 11c).

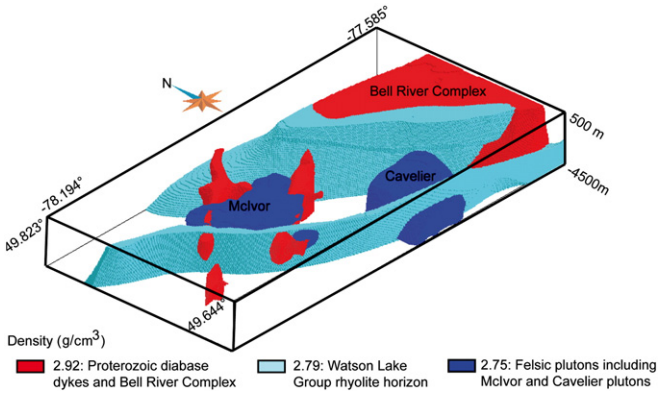

Fig. 10. 3D density model of the reference geological formations used to constrain the gravity inversion. Three different values of densities are considered for this first step, before defining the densities of the cells crosscut by drillholes.

One major difficulty for a gravity inversion is to model the extension at depth of major folded structures in the Matagami area, particularly the connection of the WLG rhyolitic horizon between the southern flank of the Galinée Anticline and the western edge of the McIvor Pluton. This would imply the existence of a synclinorium structure called the Dôme Syncline (Rhéaume, 2010). This hypothesis cannot be validated nor invalidated by our gravity modeling. The possible presence of numerous gabbroic intrusions within the rhyolitic horizon in this area would affect the gravity signal and thus lower the resolution at depth. The problem was partly solved by geological and geochemical observations of the volcanic horizons (Rhéaume, 2010) including polarity measurements, dating and rare-earth element signatures. According to these studies, the WLG rhyolitic horizon on the southern flank of the Galinée Anticline and at the western edge of the McIvor Pluton might be connected, which validates the existence of the postulated regional synclinorium. As a consequence, the so-called Dôme Syncline, might represent a huge regional structure, with strong potential targets for VMS exploration.

7. Conclusion

Two inversions of gravity anomaly have been performed in the Matagami mining camp (Abitibi Archean Subprovince) in order to follow at depth the extension of a rhyolitic horizon hosting VMS-type deposits. An unconstrained gravity inversion succeeds in generating a density model in which some low density areas are interpreted as the McIvor and Cavelier felsic plutons and the extension at depth of the Watson Lake Group rhyolitic horizon. Density measurements of representative samples of the different lithologies have been successfully cross-checked with densities calculated from their chemical compositions. These densities are incorporated in a reference density model for a constrained gravity inversion. We present several plan views of the resulting 3D density model and cross-sections are constructed to better delineate the extension at depth of the felsic plutons and rhyolitic horizon. The combination of unconstrained and constrained gravity inversion methods appears very helpful for regional mining exploration. It suggests the extension of the VMS bearing Watson Lake Group horizons along the axis of the Galinée Anticline shallowly plunging to the West and at depth along the major folds flanks. In this study, we included not only available geological information in the physical property models but also geophysical and geological interpretations. Our method leads to a geologically meaningful geo-density model of the Matagami Camp and could be extended to other areas of interest. As a backscattered effect, geophysical inversion can upgrade the geological information, as in the case of the geometry and composition of the McIvor Pluton. Additional progress in inversion methods could come from the use of more detailed reference geological models based on deep exploration drillholes for instance proving the presence at depth of the Dôme Syncline.

Acknowledgments

The present study was conducted during a one year internship of Pierre Boszczuk at MRNF in 2008–2009 and is part of a Master of Science degree obtained at the Nancy Université, France in 2010. This paper corresponds to the contribution number BEGQ-8439-2011–2012-5. Robert Marquis, Director of Géologie Québec and Sylvain Lacroix, Director of BEGQ are warmly thanked for their support. Denis Bois, Director of the Unité de Recherche et de Service en Technologie Minérale (URSTM) at the Université du Québec en Abitibi-Témiscamingue (UQAT) is acknowledged for his administrative contribution and support during the stay of Pierre Boszczuk in Québec.

Table 3
List of the main geological elements used in the reference density model with density estimation, methods for density estimation, and geological and geophysical parameters used to constrain their 3D morphology.

Geological object	Density (g/cm^3)	Density determination method	Constrains for morphology estimation
Bell River Complex	2.92	Mean of 51 known density points, inside the corresponding surface of the 2008 MRNF geological map and located upper the 50 m depth level.	Located under the Watson Lake Group rhyolitic horizon in the Southern side of Galinée Anticline. The location on surface of the contact with the Watson Lake Group rhyolitic horizon is deduced from the 2008 MRNF geological map. Contact dipping 45° SW on the southern flank of the Galinée Anticline and dipping 80° N on the northern flank (Piché, 1991).
Cavelier Pluton	2.75	McIvor and other Abitibian volcanic subprovince felsic plutons density analogy (Lacroix et al., 1990).	Pluton's limits from Goutier and Melançon (2007). Deep extension approached by the isodensity surface 2.87 g/cm^3 from the density model resulting of the unconstrained inversion.
Daniel Fault	–	–	Fault located from the Hammouche et al. (2010) and Rhéaume (2010) geological maps. Reverse fault, highly dipping to the NE, with a 500 m vertical throw, as calculated from seismic reflection interpretation (Adam et al., 1998)
Dôme Syncline	–	–	Axis located from the Rhéaume (2010) geological map. The lithological horizons located on the western edge of the McIvor Pluton (as the Watson Lake Group rhyolitic horizon) are highly dipping to the NE.
Galinée Anticline	–	–	Axis located from the Hammouche et al. (2010) and Rhéaume (2010) geological maps. The Galinée Anticline is dipping 80° N on its northern flank and 45° SW on its southern flank (Piché, 1991).
McIvor Pluton	2.75	Mean value of the density obtained by interpolation of 107 known density points inside the corresponding surface of the 2008 MRNF geological map.	Pluton's limits of the 2008 MRNF geological map. Proterozoic dykes intrusion. Deep extension approached by the isodensity surface 2.87 g/cm^3 from the density model resulting of the unconstrained inversion.
Proterozoic diabase dykes	2.92	Mean of 250 known density points, inside the corresponding surface of the 2008 MRNF geological map and located upper the 50 m depth level.	Dykes' limits of the 2008 MRNF geological map. Deep extension approached by the relative magnetic isosusceptibility surface 0.001 from the magnetic susceptibility model resulting of the unconstrained inversion.
Watson Lake Group rhyolitic horizon	2.79	Mean of 96 known density points, inside the corresponding surface of the 2008 MRNF geological map and located upper the 50 m depth level.	Horizon's limits of the 2008 MRNF geological map for the southern flank of the Galinée Anticline and of the Goutier and Melançon regional geological map (2007) for the western edge of the McIvor Pluton. On the northern flank of the Galinée Anticline, the constructed horizon is dipping 80° N (Piché, 1991). On the southern flank, the horizon has a 45°SW dip (Piché, 1991) and raises along the Dôme Syncline (Rhéaume, 2010). The deeper part of the horizon on the southern flank of Galinée Anticline is offset 500 m deeper where crosscut by the Daniel Fault (seismic reflection interpretation, Adam et al., 1998).

The core samples, chemical analyses and databases used for the density calculations came from the Système d'Information GÉOMinière (SIGEOM)-MRNF database and were provided by Michel Allard, Xstrata Zinc and SOQUEM who are warmly thanked. The quality of an earlier version of this paper was considerably improved thanks to Edward Farrar, Bill Morris and Valeria C.F. Barbosa. Anonymous reviewers and the editors Michel Chouteau and Klaus Hollinger are also warmly thanked for their reading of the first versions of the manuscript. The authors acknowledge Paradigm for making available the Gocad® geological modeler to process the inversions of the gravity field. Further

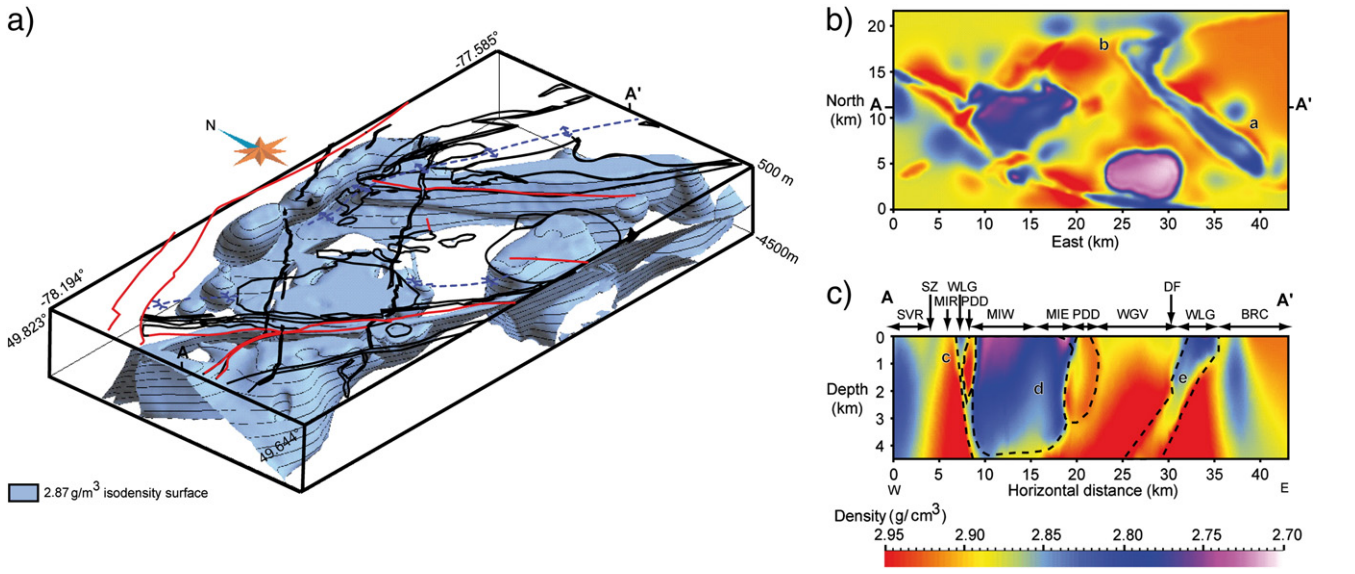

Fig. 11. a) 3D representation of the 2.87 g/cm^3 isodensity surface obtained after constrained inversion of the regional gravity anomaly. As the mean density of the studied area is 2.88 g/cm^3, this surface separates the geological objects with a higher density than 2.87 g/cm^3, supposedly mafic lithologies and andesites that provoke positive gravity anomalies, from the objects with a lower density, supposedly felsic lithologies and intermediate intrusives that provoke negative gravity anomalies. The interval between the isobath lines is 500 m. The limits of major lithologies and structures extracted from the geological map of Fig. 1 are also represented. b) Horizontal cross section at the 1 km depth. c) Vertical cross section at 49.741° latitude/78.189° longitude and 49.724° latitude/77.592° longitude. The outlines of the geological bodies as included in the reference density model are represented as dotted lines. SVR: Sedimentary and Volcanic Rocks. SZ: Shear Zone. MIR: Mafic Intrusive Rocks. WLG: Watson Lake Group rhyolitic horizon. PDD: Proterozoic Diabase Dyke. MIW: McIvor Pluton West. MIE: McIvor Pluton East. WGV: Wabassee Group Volcanic rocks. DF: Daniel Fault. BRC: Bell River Complex.

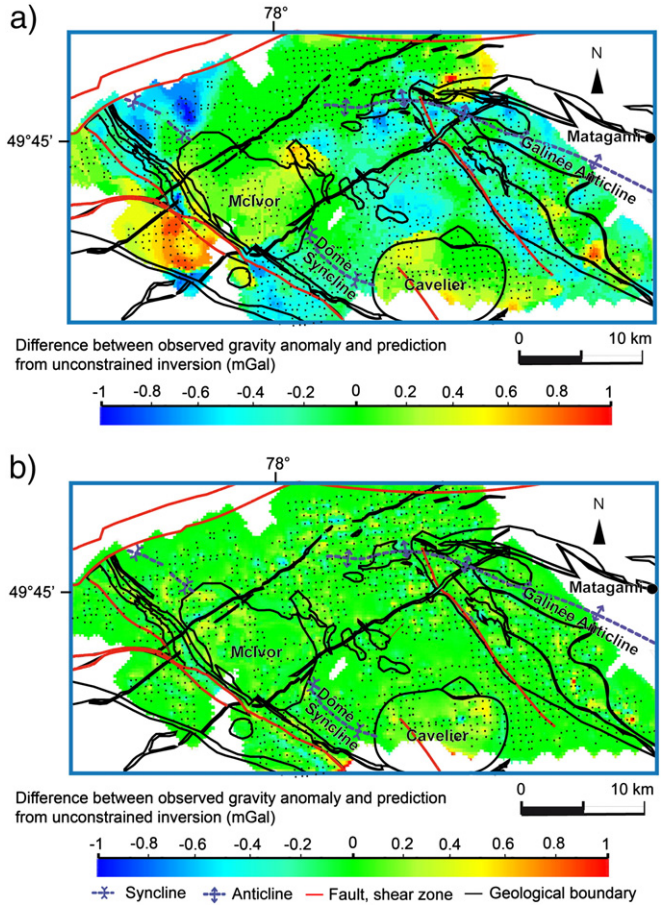

Fig. 12. a) Map of the difference between the observed gravity anomaly and the gravity anomaly predicted by the density model resulting from unconstrained inversion. b) Map of the difference between the observed gravity anomaly and the gravity anomaly predicted by the density model resulting from constrained inversion. The limits of major lithologies and structures extracted from the geological map of Fig. 1 are also represented.

details about the background theory of the software used for the presented inversions are available on the UBC-GIF website: http://www.eos.ubc.ca/ubcgif/.

References

Adam, E., Milkereit, B., Mareschal, M., 1998. Seismic reflection and borehole geophysical investigations in the Matagami mining camp. Canadian Journal of Earth Sciences 35, 686–695.

Barbosa, V.C.F., Silva, J.B.C., 1994. Generalized compact gravity inversion. Geophysics 59 (1), 57–68.

Beaudry, C., Gaucher, E., 1986. Cartographie géologique dans la région de Matagami. Ministère de l'Énergie et des Ressources du Québec MB-86-32 (in French).

Bosch, M., Meza, R., Jimenez, R., Hönig, A., 2006. Joint gravity and magnetic inversion in 3D using Monte Carlo methods. Geophysics 71, G153–G156.

Boulanger, O., Chouteau, M., 2001. Constraints in 3D gravity inversion. Geophysical Prospecting 49, 265–280.

Calvert, A., Li, Y., 1999. Seismic reflection imaging over a massive sulphide deposit at the Matagami mining camp, Québec. Geophysics 64, 24–32.

Chasseriau, P., Chouteau, M., 2003. 3D gravity inversion using a model of parameter covariance. Journal of Applied Geophysics 52, 59–74.

Daigneault, R., 1996. Couloirs de déformation de la Sous-Province de l'Abitibi. Minsitère des Ressources naturelles MB 96–33 (in French).

Farguharson, C.G., Mosher, C.M.W., 2009. Three-dimensional modelling of gravity data using finite differences. Journal of Applied Geophysics 68, 417–422.

Goutier, J., Melançon, M., 2007. Compilation géologique de la Sous-province de l'Abitibi (version préliminaire). Ministère des Ressources naturelles et de la Faune du Québec échelle 1/500 000, (map and legend, in French).

Guillen, A., Menichetti, V., 1984. Gravity and magnetic inversion with minimization of a specific functional. Geophysics 49, 1354–1360.

Hammouche, H., Roy, P., Boszczuk, P., 2008. Cartographie géologique de la région de Matagami. Ministère des Ressources naturelles et de la Faune du Québec. Quebec Exploration 2008 poster session (in French).

Hammouche, H., Boszczuk, P., Roy, P., 2010. Géologie des feuillets Ile Bancroft (32f12-200-0202) et Lac MacIvor (32f13-200-0101), région de Matagami. Ministère des Ressources naturelles et de la Faune du Québec RP 2010–01 (in French).

Lacroix, S., Simard, A., Pilote, P., Dubé, L.M., 1990. Regional geologic elements and mineral resources of the Harricana Turgeon Belt, Abitibi of NW Québec. In: Rive, M., Verpaelst, P., Gagnon, Y., Lulin, J.M., Riverin, G., Simard, A. (Eds.), The northwestern Quebec polymetallic belt; a summary of 60 years of mining exploration. Proceeding of the Rouyn-Noranda 1990 symposium: Canadian Institute of Mining and Metallurgy, Vol. 43, pp. 313–326. Special.

Last, B.J., Kubik, K., 1983. Compact gravity inversion. Geophysics 48, 713–721.

Li, Y., Oldenburg, D.W., 1998. 3-D inversion of gravity data. Geophysics 63, 109–119.

CRC Handbook of Chemistry and Physics (Internet Version) In: Lide, D.R. (Ed.), 90th Edition. CRC Press/Taylor and Francis, Boca Raton, FL.

Mallet, J.L., 1992. Discrete smooth interpolation. Computer Aided Design Journal 24 (4), 263–270.

Mortensen, J.K., 1993. U–Pb geochronology of the eastern Abitiby subprovince. Part 1: Chibougamau–Matagami–Joutel region. Canadian Journal of Earth Sciences 30, 11–28.

Piché, M., 1991. Synthèse géologique et métallogénique du camp minier de Matagami, Québec. Université du Québec à Chicoutimi. PhD thesis (in French).

Piché, M., Jebrak, M., 2004. Normative minerals and alteration indices developed for mineral exploration. Journal of Geochemical Exploration 82, 59–77.

Piché, M., Guha, J., Daigneault, R., 1993. Stratigraphic and structural aspects of the volcanic rocks of the Matagami mining camp, Quebec: implications for the Norita ore deposit. Economic Geology 88, 1542–1558.

Rhéaume, P., 2009. Cartographie de la région de la rivière Allard, ProjetMatagami, phase 2/3. Ministère des Ressources naturelles et de la Faune du Québec. Quebec Exploration 2009, poster session (in French).

Rhéaume, P., 2010. Géologie du feuillet lac Watson (32f12-200-0201), et des portions attenantes des feuillets rivière Subercase (32e09-200-0202), lac de la Gauchetière (32e16-200-0102) et lac McIvor (32f13-200-0101), région de Matagami. Ministère des Ressources naturelles et de la Faune du Québec GM 64950 (in French).

Shamsipour, P., Marcotte, D., Chouteau, M., Keating, P., 2010. 3D stochastic inversion of gravity data using cokriging and cosimulation. Geophysics 75 (1), 1–10.

Silva Dias, F.J.S., Barbosa, V.C.F., Silva, J.B.C., 2009. 3D gravity inversion through an adaptive learning procedure. Geophysics 74 (3), I9–I21.

Silva, J.B.C., Barbosa, V.C.F., 2006. Interactive gravity inversion. Geophysics 71 (1), J1–J9.

Silva, J.B.C., Medeiros, W.E., Barbosa, V.C.F., 2001. Potential field inversion: choosing the appropriate technique to solve a geologic problem. Geophysics 66 (2), 511–520.

Telford, W.M., Geldart, L.P., Sheriff, R.E., Keys, D.A., 1990. Applied Geophysics, 2nd edition. Cambridge University Press.

Veillette, J.J., Pomares, J.-S., 2003. Géologie des formations en surface et histoire glaciaire, Lac Matagami, Québec. Commission géologique du Canada Map 1994A, scale 1/100000 (in French).